

Thermodynamics of colloidal suspensions

Yoshihiro Hirata* and Yosuke Tanaka

Department of Advanced Nanostructured Materials Science and Technology, Kagoshima University, 1-21-40 Korimoto, Kagoshima 890-0065, Japan

This paper succeeds in the description of activity (a), chemical potential (μ), and their thermodynamic relations of dispersed and flocculated particles of a one-component colloidal system. The activity of dispersed particles (a_d) is expressed by Henry's law and equal to the product of the molar fraction (α) of dispersed particles in a suspension and the activity coefficient (γ^0) expressed by V_i/V_{\max} (V_i : total volume fraction of dispersed and flocculated particles, V_{\max} : maximum packing density of particles). The activity of flocculated particles (a_g) follows Raoult's law and is expressed as $(1 - \alpha)$ using the Gibbs-Duhem equation. The μ value is represented by the defined activity. The difference of μ for the dispersed and flocculated particles ($\Delta\mu = \mu_g - \mu_d$) was used to evaluate the stability of the colloidal state. The $\Delta\mu$ value was also coupled with the activation energy (ΔG_m) for the formation of particle clusters from the dispersed state. The enthalpy term (ΔH_m) in the activation energy is equivalent to the maximum value of the interaction energy ($E_i(\max)$) as a function of distance between two particles in the DLVO theory. Based on the above analysis, a colloidal phase diagram for one-component systems of 10-1000 nm diameters was constructed. This phase diagram explains well the experimentally-determined packing density for dispersed and flocculated suspensions.

Key words: Thermodynamics, Colloidal suspension, Phase diagram, Packing density, Dispersion, Flocculation, Activity, Chemical potential.

Introduction

Powder processing through colloidal suspensions is widely recognized to be a forming method which can improve the microstructure and the resultant physicochemical properties of advanced ceramics [1-6]. The guideline of colloidal processing is given by the interaction energy between charged particles, which corresponds to the summation of van der Waals attraction energy and the electrostatic repulsive energy by the electrical double layer (DLVO theory) [7-10]. The DLVO theory explains the dispersed and flocculated state depending on the surface potential of the particles. Based on the DLVO theory, we constructed a metastable phase diagram of a one-component colloidal system in the map of surface potential and solid content of particles to understand the particle size effect on the stability of a colloidal suspension [9, 11, 12]. This phase diagram is effective to understand the properties of a colloidal suspension of nanometre-sized particles. Aksay and Kikuchi propose a phase diagram for a one-component colloidal system of monosize spherical particles, calculated by the cluster variation method (CVM) based on a two dimensional lattice gas model [4, 13]. This phase diagram shows the stability regions of colloidal gas, liquid and solid phases and

outlined with the theoretically reduced temperature $k(B)T/E_i$ and solid content, where $k(B)$ is the Boltzmann constant, T is the thermodynamic temperature, and E_i is the interaction energy between particles. Russel also reports an equilibrium phase diagram of one-component colloidal system [14]. Both these phase diagrams are basically the same and helpful to control the nature of colloidal suspensions and to predict resultant microstructures of consolidated powder compacts. Deniz et al. [15] have reported colloidal phase diagrams calculated from first order perturbation theory for three different aqueous aluminium oxide nanoparticle suspensions containing non-polarizable salt, NaCl or NaI. Zamora and Zukoski [16], and Ramakrishnan and Zukoski [17] show phase diagrams calculated by perturbation theory using the Yukawa potential for nanoparticle suspensions. These phase diagrams in references 15-17 for nanoparticle suspensions are similar to the phase diagrams previously reported in references 13 and 14.

For more understanding of the properties of colloidal suspension, we need a description of the thermodynamics of colloidal systems, which may be used as a guideline of colloidal processing. Unfortunately, no paper has established the thermodynamics of colloidal suspensions and described the relationship between the colloidal phase diagram and thermodynamics. In this paper, we propose a simple suspension model and discuss the thermodynamics of the suspension. From the derived thermodynamic relations, we have constructed a one-component colloidal phase diagram and compared with

*Corresponding author:
Tel : +81-99-285-8325
Fax: +81-99-257-4742
E-mail: hirata@apc.kagoshima-u.ac.jp

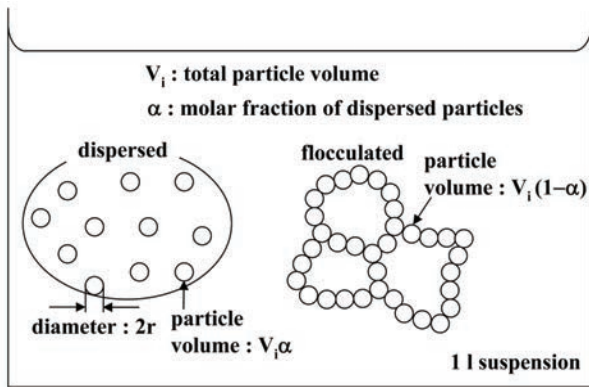


Fig. 1. A suspension model containing dispersed particles and flocculated particles.

the previously reported phase diagrams. The constructed phase diagram also succeeded in a quantitative explanation of the dependence of packing density of colloidal particles on particle size. This type of colloidal phase diagram is useful to predict the flow behavior of a colloidal suspension and the phase transition from colloidal liquid to colloidal solid in ceramic processing. Much time can be saved by reference to a phase diagram in the forming of ceramic particles with different sizes or different surface chemistries.

Definition of Activity and Chemical Potential

Figure 1 shows a structure model of colloidal suspension (1 l volume) containing both dispersed and flocculated particles. The suspension contains n_i spherical particles of radius r . The total volume of n_i particles is $V_i = n_i v_i$ ($v_i = 4\pi r^3/3$, volume of one particle). The volume of dispersed (V_d) and flocculated (V_g) particles is $V_i \alpha$ and $V_i (1 - \alpha)$, respectively, where α is the molar fraction (volume fraction) of dispersed particles to the total particle content. The concentration (mol/l) of dispersed (C_d) and flocculated (C_g) particles is also defined to be $n_i \alpha / n_A$ ($= V_i \alpha / v_i n_A$, n_A : Avogadro number) and $n_i (1 - \alpha) / n_A$, respectively. The activity of dispersed particles (a_d) is defined by Eq. (1) [18]:

$$a_d = X_d \gamma_d^0 = \left(\frac{C_d}{C_d + C_g} \right) \gamma_d^0 = \alpha \gamma_d^0 \quad (1)$$

where X_d and γ_d^0 are the molar fraction and activity coefficient of dispersed particles, respectively. According to the definition of activity ($0 < \alpha < 1$, $X_d \rightarrow 1$, $a_d \rightarrow 1$), γ_d^0 should become 1 at $\alpha = 1$. The above condition leads to the relation of $\gamma_d^0 = V_i / V_{\max}$, where V_{\max} is the maximum volume of particles packed in 1 l suspension. For the close packing and random close packing models [19], V_{\max} is 0.740 and 0.637 l, respectively. The γ_d^0 value results in 1 for $V_i = V_{\max}$. That is, a_d is defined as a ratio of the volume of dispersed particles to the maximum volume packed, $a_d = V_i \alpha / V_{\max} = V_d / V_{\max}$. When a colloidal suspension is prepared at a certain volume fraction (V_i), the activity of dispersed particles is smoothly given

by Eq. (1). This relation is known as Henry's law [18].

Since the activity of dispersed particles can be defined by Henry's law, the activity of flocculated particles (a_g) is derived using the Gibbs-Duhem equation [18], $X_d \ln a_d + X_g \ln a_g = 0$ ($X_g = 1 - \alpha$: molar fraction of flocculated particles). When a_d is described by Henry's law, a_g is equal to X_g , which is known as Raoult's law [18]. That is:

$$a_g = X_g = 1 - \alpha \quad (2)$$

The flocculated particles behave as an ideal solution. The activity of dispersed and flocculated particles (Eqs. (1) and (2)) is related to the chemical potential as follows:

$$\mu_d(\text{dispersed}) = \mu_{d0} + RT \ln a_d = \mu_{d0} + RT \ln \gamma^0 \alpha \quad (3)$$

$$\mu_g(\text{flocculated}) = \mu_{g0} + RT \ln a_g = \mu_{g0} + RT \ln (1 - \alpha) \quad (4)$$

The μ_{d0} value represents the chemical potential of dispersed particles for $\alpha = 1$ and $\gamma^0 (= V_i / V_{\max}) = 1$. Similarly, the μ_{g0} corresponds to the chemical potential of flocculated particles for $\alpha = 0$. The difference of chemical potential of both the particles is expressed by Eq. (5):

$$\Delta\mu = \mu_g - \mu_d = \Delta\mu_0 + RT \ln \left(\frac{1 - \alpha}{\gamma^0 \alpha} \right) \quad (5)$$

where $\Delta\mu_0$ represents $\mu_{g0} - \mu_{d0}$. The condition of $\Delta\mu > 0$ indicates the change of flocculated particles to dispersed particles. On the other hand, dispersed particles change to flocculated particles at $\Delta\mu < 0$. The dispersed and flocculated state reaches an equilibrium at $\Delta\mu = 0$. The critical fraction (α_c) of dispersed particles at $\Delta\mu = 0$ is given by Eq. (6):

$$\alpha_c = \frac{1}{1 + \gamma^0 \exp\left(-\frac{\Delta\mu_0}{RT}\right)} \quad (6)$$

Change of Dispersed to Flocculated State

The dispersed particles in a suspension collide to form flocculated particles. The collision rate is usually expressed by a second order reaction (Eq. (7)) [7, 8]:

$$-\frac{dC_d}{dt} = k C_d^2 \quad (7)$$

where k is the rate constant. This equation is easily solved under the conditions of $C_d = n_d / n_A$ at $t = 0$ and $C_d = n_d / n_A$ at $t = t$, where n_d is the number of dispersed particles ($n_d = n_i \alpha$). The integrated form is given by Eq. (8):

$$\frac{1}{n_d} - \frac{1}{n_i} = \frac{1}{n_i \alpha} - \frac{1}{n_i} = \left(\frac{k}{n_A} \right) t \quad (8)$$

From Eq. (8), α is expressed by Eq. (9):

$$\alpha = \frac{1}{1 + n_i k_1 t} \quad (9)$$

where k_1 is equal to k/n_A . That is, the fraction of dispersed particles is a function of settling time and decreases at a longer time. Equation (9) is coupled with Eqs. (1)-(5) to represent the activity and chemical potential of particles in a suspension as a function of settling time (Eqs. (10)-(14)):

$$a_d = \gamma^0 \alpha = \gamma^0 \left(\frac{1}{1 + n_i k_1 t} \right) \quad (10)$$

$$\mu_d = \mu_{d0} + RT \ln \gamma^0 \alpha = \mu_{d0} + RT \ln \gamma^0 - RT \ln (1 + n_i k_1 t) \quad (11)$$

$$a_g = 1 - \alpha = \frac{n_i k_1 t}{1 + n_i k_1 t} \quad (12)$$

$$\mu_g = \mu_{g0} + RT \ln (1 - \alpha) = \mu_{g0} + RT \ln \left(\frac{n_i k_1 t}{1 + n_i k_1 t} \right) \quad (13)$$

$$\Delta\mu = \Delta\mu_0 + RT \ln \left(\frac{1 - \alpha}{\gamma^0 \alpha} \right) = \Delta\mu_0 - RT \ln \gamma^0 + RT \ln (n_i k_1 t) \quad (14)$$

Figure 2 shows the schematic relation of a and μ as a function of time. The a_d decreases from γ^0 at $t = 0$ to 0 at $t = \infty$. On the other hand, the a_g increases from 0 at $t = 0$ to 1 at $t = \infty$. This change is accompanied by the change in μ_g from $-\infty$ at $t = 0$ to μ_{g0} at $t = \infty$. The important note is that the collision of dispersed particles stops at a critical time t_{c1} for $\Delta\mu = 0$, because the equilibrium state is achieved. The time t_{c1} required to reach the equilibrium

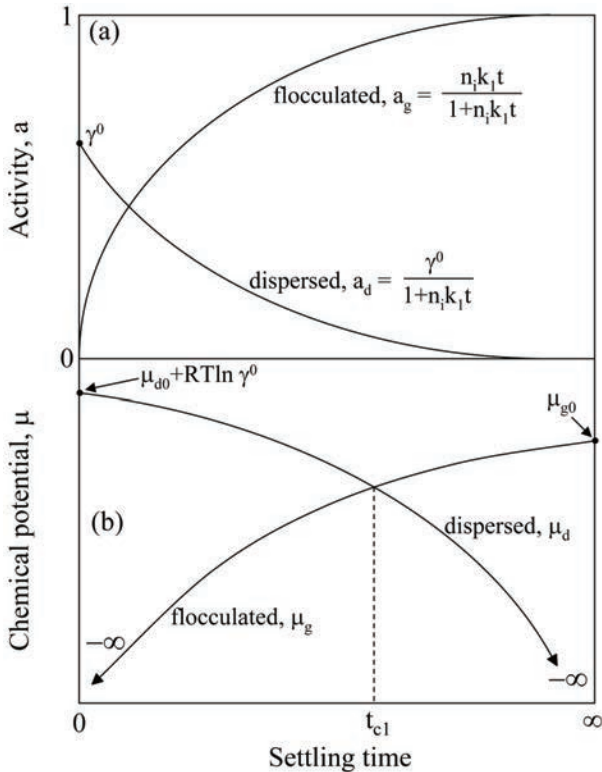


Fig. 2. Schematic relation of activity (a) and chemical potential (b) of dispersed and flocculated particles as a function of settling time.

state is determined from Eq. (14):

$$t_{c1} = \frac{\gamma^0}{n_i k_1} \exp \left(\frac{\Delta\mu_0}{RT} \right) \quad (15)$$

The molar fraction of α at $t = t_{c1}$ is also determined from Eqs. (9) and (15) as follows :

$$\alpha_c (\text{for dispersed particles}) = \frac{\exp \left(\frac{\Delta\mu_0}{RT} \right)}{\gamma^0 + \exp \left(\frac{\Delta\mu_0}{RT} \right)} \quad (16)$$

$$1 - \alpha_c (\text{for flocculated particles}) = \frac{\gamma^0}{\gamma^0 + \exp \left(\frac{\Delta\mu_0}{RT} \right)} \quad (17)$$

Equation (16) is the same as Eq. (6). The chemical potential of μ_d and μ_g at $t = t_{c1}$ is given by Eq. (18):

$$\mu_g = \mu_d = \mu_{g0} + RT \ln \gamma^0 - RT \ln \left(\gamma^0 + \exp \left(\frac{\Delta\mu_0}{RT} \right) \right) \quad (18)$$

When $n_i k_1$ in Eq.(14) is substituted for $n_i k_1$ in Eq. (15), the $\Delta\mu$ value is expressed as a function of t/t_{c1} ratio (Eq. (19)):

$$\Delta\mu = RT \ln \left(\frac{t}{t_{c1}} \right) \quad (19)$$

The $\Delta\mu$ value becomes $\Delta\mu < 0$ at $t < t_{c1}$ and $\Delta\mu = 0$ at $t = t_{c1}$. No change of $\Delta\mu$ occurs at $t > t_{c1}$, because the equilibrium state is achieved.

Particle Size Effect on the Phase Transition from Dispersed to Flocculated State

The fraction (α) of dispersed particles at time t depends on the rate constant k_1 in Eq. (9). The rate constant is expressed by an Arrhenius equation Eq. (20) [7, 20]:

$$k_1 = k_{10} \exp \left(- \frac{\Delta G_{m1}}{RT} \right) \quad (20)$$

where k_{10} is the frequency factor and ΔG_{m1} represents the activation energy for the migration of a dispersed particle to another dispersed particle or to an adjacent flocculated particle. The critical time t_{c1} for the phase transition from the dispersed to flocculated state is expressed as follows by the combination of Eqs. (15) and (20) :

$$t_{c1} = \frac{\gamma^0}{n_i k_{10}} \exp \left(- \frac{\Delta\mu_0 - \Delta G_{m1}}{RT} \right) \quad (21)$$

Figure 3 shows the energy difference of dispersed and flocculated particles at $t < t_{c1}$ and $t = t_{c1}$. The dispersed particles form a particle cluster when they have an energy higher than the potential barrier, ΔG_{m1} . Although μ_d of dispersed particles is higher than μ_g of flocculated particles at $t < t_{c1}$, it is difficult to form particle clusters because of a high potential barrier, resulting in a long t_{c1} time. For the dispersion of flocculated particles, more energy ($\Delta G_{m1} - \Delta\mu$)

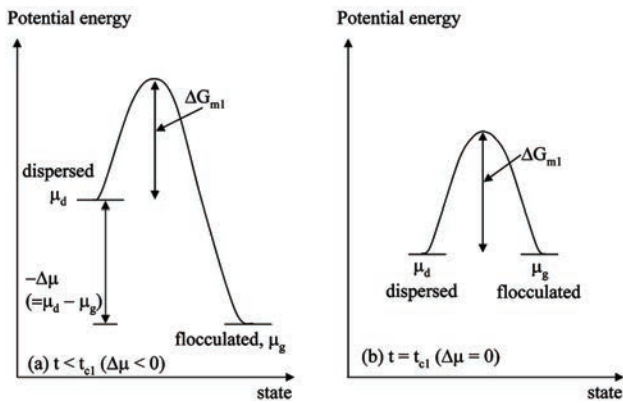


Fig. 3. Energy difference of dispersed and flocculated particles at (a) $t < t_{c1}$ (critical time for equilibrium) and (b) $t = t_{c1}$. ΔG_{m1} represents the activation energy for one particle to migrate to another particle.

is required at $t < t_{c1}$. Once the equilibrium is reached ($\Delta\mu = 0$), the numbers of particles migrating for 1 second in both the directions of dispersed \rightarrow flocculated and flocculated \rightarrow dispersed become the same, indicating constant numbers of dispersed and flocculated particles in a suspension.

Equation (21) is transformed to Eq. (22) using the basic relations of $\gamma_0/n_i = (V_i/V_{max})$ ($v_i/V_i = 4\pi r^3/3V_{max}$), $\Delta\mu_0 = \Delta H_0 - T\Delta S_0$ and $\Delta G_{m1} = \Delta H_{m1} - T\Delta S_{m1}$ (H : enthalpy, S : entropy, T : temperature):

$$\ln t_{c1} = \ln \left(\frac{4\pi}{3V_{max}k_{10}} \right) + 3 \ln r - \frac{\Delta S_{m1} - S_0}{R} - \frac{\Delta H_0}{RT} + \frac{\Delta H_{m1}}{RT} \quad (22)$$

In Eq. (22), the entropy difference (ΔS_0) of dispersed and flocculated particles at $a_d = a_g = 1$ should be close to ΔS_{m1} of the dispersed and flocculated particles present at $t = t$, leading to $\Delta S_{m1} - \Delta S_0 \approx 0$. That is, Eq.(22) is simply expressed by Eq. (23):

$$\ln t_{c1} \approx A + 3 \ln r + \frac{\Delta H_{m1}}{RT} \quad (23)$$

where A has a constant value ($\ln(4\pi/3V_{max}k_{10}) - \Delta H_0/RT$). Equation (23) indicates that (i) t_{c1} depends on particle size and ΔH_{m1} (enthalpy for migration of a dispersed particle) and (ii) t_{c1} becomes longer for a larger r and for a higher ΔH_{m1} value.

Stability of Dispersed Particles

Colloidal processing needs well dispersed particles to make a dense powder compact [12]. The stability of the colloidal suspension is an important factor in actual processing. The thermodynamic condition for stable dispersed particles is given by $\Delta\mu/RT < 0$ ($\mu_g < \mu_d$). In this condition, we can get a colloidal suspension containing well-dispersed particles rather than flocculated particles. In particular, the difference of chemical potential ($\Delta\mu$)

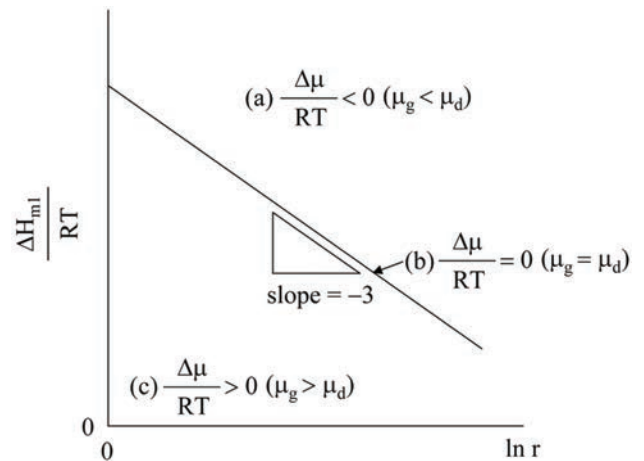


Fig. 4. Relation between particle size and enthalpy for the migration of dispersed particles to form a particle cluster.

is large for a short settling time (fresh suspension) as seen in Fig. 2 and Eq. (14). From Eq. (19), the following relation is derived for $t_{c1} > t > 1$ second:

$$\frac{\Delta\mu}{RT} - \ln t = -\ln t_{c1} < -\ln t < 0 \quad (24)$$

Equation (24) indicates that the suspension with a long t_{c1} has a large difference of chemical potential at a similar settling time. Therefore, $-\ln t_{c1}$ is a possible indicator for the stability of dispersed colloidal particles. When $\ln t_{c1}$ is large with a negative value, the suspension contains more dispersed particles. From Eqs. (23) and (24), $-\ln t_{c1}$ for a fresh suspension ($\ln t \ll \ln t_c$) is expressed by Eq. (25):

$$\frac{\Delta\mu}{RT} \approx -\ln t_{c1} \approx -A - \frac{\Delta H_{m1}}{RT} - 3 \ln r < 0 \quad (25)$$

Figure 4 shows the schematic relation between $\Delta H_{m1}/RT$ value and $\ln r$ for Eq.(25). A large ΔH_{m1} provides a high stability of the colloidal suspension. The critical ΔH_{m1} for $\Delta\mu/RT = 0$ increases linearly with decreasing $\ln r$. This relation suggests that the activation energy (ΔH_{m1}) to prevent the formation of a particle cluster by collision of dispersed particles is a function of particle size and should increase when the particle size becomes small. For a similar ΔH_{m1} value, large particles are well dispersed but small particles are flocculated.

Phase Diagram of One-Component Colloidal System

In section 5, we discussed the stability of a colloidal suspension. For a fresh suspension ($\ln t \ll \ln t_c$), the stability factor, $-\ln t_c$, is approximated to $\Delta\mu/RT$ (See Eqs. (19) and (25)). To make a stable dispersed suspension, the ΔH_{m1} in Eq. (25) value is discussed in this section. The ΔH_{m1} value for dispersed particles is an enthalpy to make a particle cluster. This value can be calculated by DLVO theory. Figure 5 shows the interaction energy (E_i)

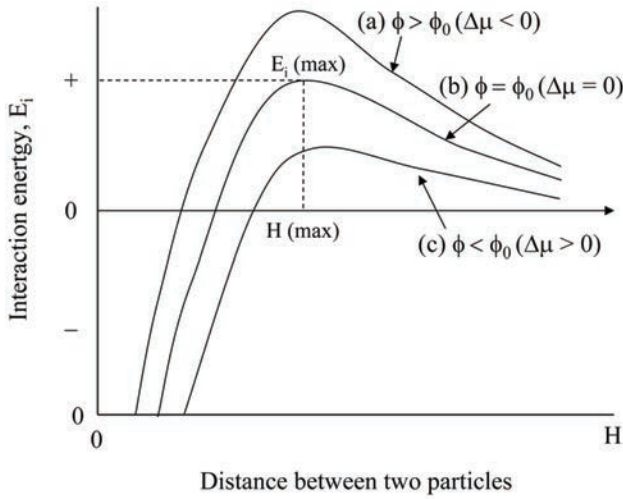


Fig. 5. Schematic relation of the interaction energy between two particles as a function of their distance. ϕ is a surface potential.

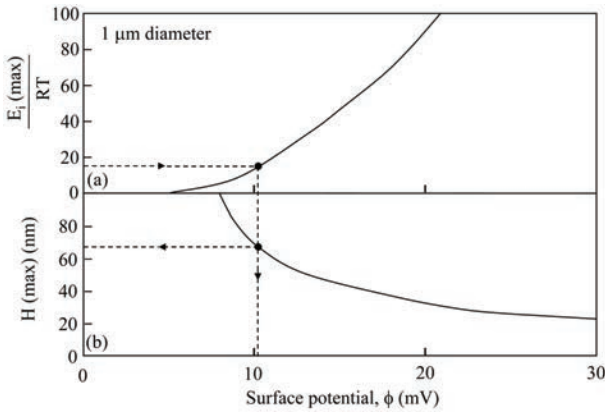


Fig. 6. Maximum value of interaction energy (a) and corresponding particle distance (b) for 1 μm particles as a function of surface potential.

as a function of distance between two dispersed particles. The E_i value is a summation of the van der Waals attraction energy (E_a) and the repulsive energy (E_r) due to overlap of the electrical double layer between two charged particles. The maximum value of E_i ($E_i(\text{max})$) depends on the surface potential of dispersed particles when the particle size and concentration of electrolyte of a suspension are fixed. A certain $E_i(\text{max})$ corresponds to a critical ΔH_{m1} value which is equal to $RT(-A-3 \ln r)$ in Eq. (25). Once a critical $\Delta H_{m1}/RT$ value for a particle radius r_1 is given, the other critical $\Delta H_{m1}/RT$ value for a different particle radius r_2 is easily determined using Eq. (26) derived from Eq. (25):

$$\frac{\Delta H_{m1} \text{ for } r_2}{RT} = \frac{\Delta H_{m1} \text{ for } r_1}{RT} + 3 \ln \left(\frac{r_1}{r_2} \right) \quad (26)$$

However, it is difficult to determine the theoretical A value in Eq. (25), because two unknown parameters k_{10} and ΔH_0 are included in the A value (See Eqs. (22) and (23)). As a starting point, an experienced criterion of $\Delta H_{m1}(\text{critical})/RT \approx 15$ was assumed for a particle of 1 μm diameter [10]. The $E_i(\text{max})$ was calculated for

many surface potential ϕ mV under the constant conditions of an electrical double layer thickness = 100 nm, Hamaker constant 10.7×10^{-20} J, atomic valence of electrolyte in a suspension +1 and temperature 298 K. The detailed E_a and E_r equations are shown in our previous paper [10]. Equations (27), (28) and (29) represent for E_a , E_r for D (particle diameter) $\gg 1/\kappa$ (double layer thickness) and E_r for $D \ll 1/\kappa$, respectively :

$$E_a = -\frac{A(H)}{12} \left[\frac{D^2}{H^2 + 2DH} + \frac{D^2}{(H+D)^2} + 2 \ln \frac{H^2 + 2DH}{(H+D)^2} \right] \quad (27)$$

$$E_r = 32\pi\epsilon\epsilon_0 \left(\frac{D}{2} \right) \left(\frac{k(B)T}{Ze} \right)^2 \left[\frac{\exp \left(\frac{Ze\phi}{2k(B)T} \right) - 1}{\exp \left(\frac{Ze\phi}{2k(B)T} \right) + 1} \right]^2$$

$$\ln[1 + \exp(-\kappa H)] = 32\pi\epsilon\epsilon_0 \left(\frac{D}{2} \right) \left(\frac{RT}{ZF} \right)^2 \tan^2 h^2 \left(\frac{ZF\phi}{4RT} \right)$$

$$\ln[1 + \exp(-\kappa H)] \quad (D \gg 1/\kappa) \quad (28)$$

$$E_r = \frac{\pi\epsilon\epsilon_0 D^2 \phi^2}{H+D} \exp(-\kappa H) \quad (D \ll 1/\kappa) \quad (29)$$

$A(H)$ in Eq. (27) is the Hamaker constant and the value of $A(H) = 10.7 \times 10^{-20}$ J for SiC particles was used in present calculation. H is the distance between two particles, $k(B)$ the Boltzmann constant, ϵ the relative dielectric constant of H_2O (78.3), ϵ_0 the permittivity of vacuum (8.854×10^{-12} F/m), R the gas constant (8.314 J/mol K), T the temperature, Z the charge number (assumed to be +1) of the electrolyte and F the Faraday constant (9.649×10^4 C/mol). The double layer thickness of 100 nm was calculated for a typical concentration (10^{-5} mol/l) of the electrolyte of $Z = 1$.

Figure 6 shows the calculated $E_i(\text{max})/RT$ value and corresponding particle distance $H(\text{max})$ as a function of surface potential ϕ for the particles of 1 μm diameter. In this figure, the surface potential for the critical value of $\Delta H_{m1}/RT = E_i(\text{max})/RT = 15$ was determined to be 10.3 mV. The $H(\text{max})$ value was also determined to be 67 nm. A similar method was used to determine the other critical ϕ and $H(\text{max})$ values for different particle sizes. The critical $\Delta H_{m1}/RT$ values calculated by Eq. (26) are 17.1 for 500 nm diameter, 21.9 for 100 nm diameter, 22.6 for 80 nm diameter, 23.4 for 60 nm, 25.5 for 30 nm diameter and 28.8 for 10 nm diameter. The critical $\Delta H_{m1}/RT$ value increases with decreasing particle size. Of course, when a theoretical A value in Eq. (25) is determined, we can discuss a more accurate particle size dependence of the critical value $\Delta H_{m1}/RT$. Figure 7 shows, $\Delta\mu / RT$ ($\approx -\ln t_c$ for a fresh suspension) as a function of $\Delta H_{m1}/RT$. The chemical potential of dispersed particles with ϕ higher than ϕ_0 (critical surface potential) in a fresh suspension is higher than the chemical potential of flocculated particles. The $\Delta\mu/RT$ ($-\ln t_c$) approaches 0

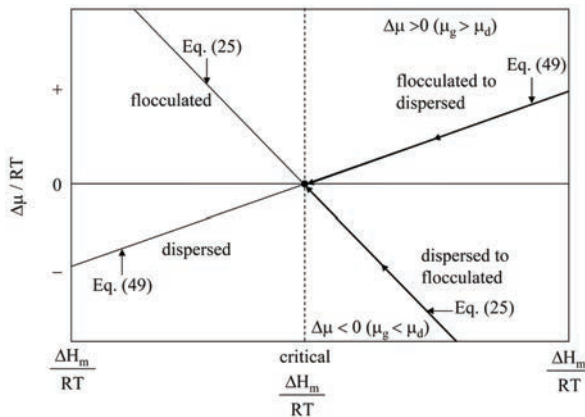


Fig. 7. Relationship between $\Delta\mu/RT$ and $\Delta H_m/RT$ for the phase transition from dispersed to flocculated particles and from flocculated to dispersed particles. See Eqs. (25) and (49) in the text for the criterion of the dispersion of colloidal particles.

at a critical ϕ_0 value. In the range $\phi < \phi_0$, the chemical potential of flocculated particles becomes higher than that of dispersed particles. The thermodynamics in this range is discussed more in section 8. That is, surface potential of particles should be higher than ϕ_0 to make a well dispersed suspension. On the other hand, the $H(max)$ in Fig. 6 was converted to the initial concentration of colloidal particles V_i (see section 2), using Eq. (30) for random close packing model [21, 22]:

$$H(max) = 2r \left[\left(\frac{1}{3\pi V_i} + \frac{5}{6} \right)^{\frac{1}{2}} - 1 \right] \quad (30)$$

The $H(max)$ value approaches 0 at $V_i = 63.7$ vol%. As seen in Fig. 5, two dispersed particles within a distance of $0 < H < H(max)$ have a strong tendency to make a particle cluster because of the rapid decrease of E_i to $-\infty$ with decreasing H value. That is, the increasing solid content of the well-dispersed colloidal suspension ($\phi > \phi_0$) leads to the consolidation of colloidal particles (formation of a dense powder compact). Therefore, three different phases are present in a one-component colloidal system: a colloidal suspension containing well-dispersed particles ($\Delta\mu/RT < 0$, $\phi > \phi_0$, $H > H(max)$, named as colloidal liquid), a dense powder compact consolidated from well-dispersed particles ($\Delta\mu/RT < 0$, $\phi > \phi_0$, $H = 0$, named as colloidal solid), a colloidal suspension containing flocculated particles ($\Delta\mu/RT > 0$, $\phi < \phi_0$, named a flocculated suspension). In the distance range of $0 < H < H(max)$, two phases (colloidal liquid and colloidal solid) coexist. Based on the above discussion, the phase diagram of a fresh colloidal suspension ($\ln t \ll \ln t_c$) was constructed for many particle sizes.

Figure 8 shows the colloidal phase diagram of a fresh suspension containing 1 μm particles. The phase transition from a colloidal liquid to a flocculated suspension occurs at $\phi = 10.3$ mV. The flocculated suspension formed consists of two phases of flocculated colloidal particles and an aqueous solution. Therefore, the phase transition at $\phi = \phi_0$

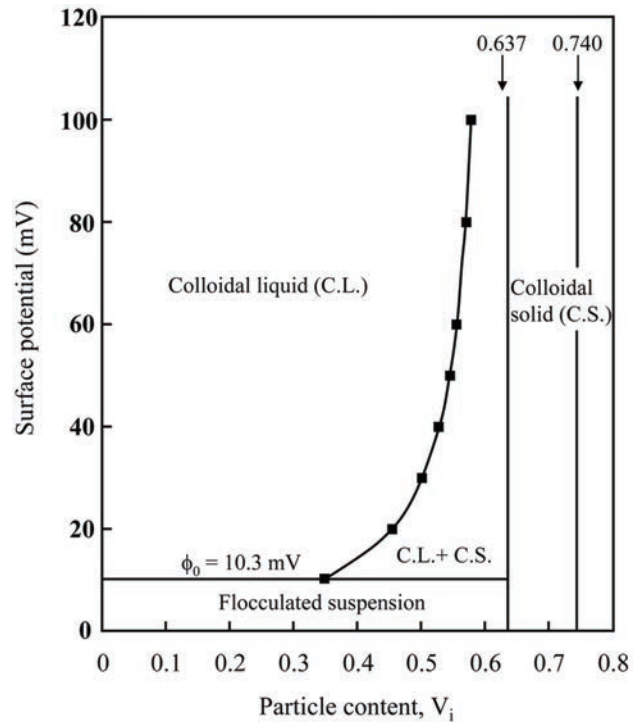


Fig. 8. Colloidal phase diagram of one-component system of 1 μm particles.

is accompanied by the phase separation from one phase (colloidal liquid) to two phases (flocculated particles and aqueous solution). On the other hand, the V_i range for the mixture of colloidal liquid and colloidal solid becomes narrow at a higher ϕ value ($\phi > \phi_0$). The phase diagram suggests a concentrated suspension of 55 vol% particles may be prepared at $\phi > 60$ mV. The phase diagram obtained is essentially same as the phase diagrams reported by Aksay and Kikuchi [4, 13], and Russel [14]. The thermodynamics of colloidal suspension discussed is drawn in one phase diagram. The phase diagram of Fig. 8 for a fresh suspension was compared with the metastable phase diagram in our previous papers [9, 11, 12]. When the definition of the colloidal state in the previous paper is changed from colloidal solid to colloidal solid + colloidal liquid, and from colloidal solid + colloidal liquid to colloidal liquid, both the phase diagrams are essentially equivalent. Figure 9 compares the colloidal phase diagrams for the particle size range from 1 μm to 10 nm. The critical surface potential ϕ_0 increases with decreasing particle size. This result has been discussed in section 5 and related to the particle size dependence of the critical ΔH_{m1} value (Eqs. (25) and (26)). In an actual processing, a higher ϕ is required for nanometre-sized particles to make a well-dispersed fluid suspension. The V_i range for the mixture of colloidal liquid plus colloidal solid becomes wide with decreasing particle size. In this V_i range, it is difficult to change the position of particles, because the distance between two particles is substantially shorter than the particle size. The above comparison suggests the consolidation of fine particles results in a low packing density.

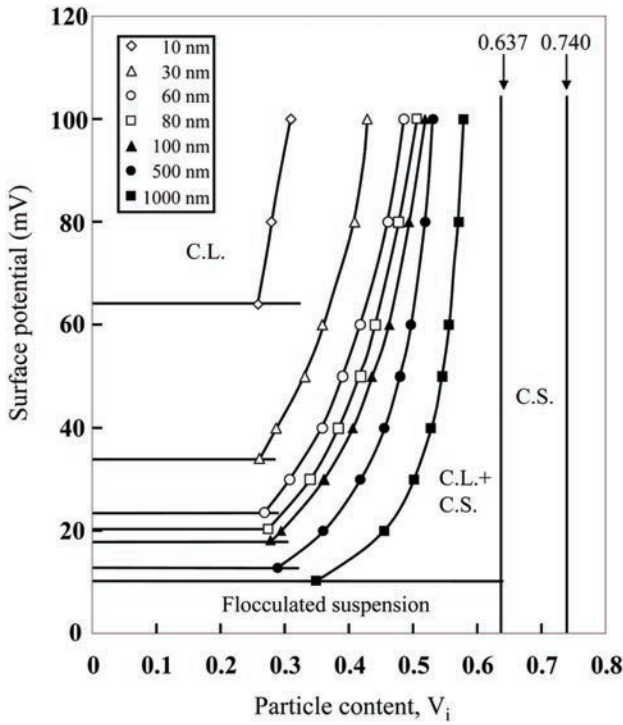


Fig. 9. Comparison of colloidal phase diagrams for particle size range from 1 μm to 10 nm.

Change of the Flocculated to the Dispersed State

In this section, we discuss the dispersion of flocculated particles at $\phi < \phi_0$. The number of particles released from flocculated particles per unit area for 1 second is expressed by Eq. (31) [23]:

$$\frac{dC_d}{dt} = -\frac{dC_g}{dt} = k_2(C_g - C_d) \quad (31)$$

where k_2 is the rate constant. Since C_d and C_g are equal to $V_i \alpha / v_i n_A$ and $V_i (1 - \alpha) / v_i n_A$, respectively, Eq. (31) is transformed to Eq. (32):

$$\frac{d\alpha}{dt} = k_2(1 - 2\alpha) \quad (32)$$

Equation (32) is integrated under the consolidations of $\alpha = 0$ at $t = 0$ and $\alpha = \alpha$ at $t = t$. The solved form is given by Eq. (33):

$$-\ln(1 - 2\alpha) = 2k_2 t \quad (33)$$

The molar fraction of dispersed particles is expressed by Eq. (34):

$$\alpha = \frac{1}{2}(1 - \exp(-2k_2 t)) \quad (34)$$

The α value increases from 0 at $t = 0$ to 0.5 at $t = \infty$. The activity of dispersed and flocculated particles is as follows :

$$a_d = \gamma^0 \alpha = \frac{\gamma^0}{2}(1 - \exp(-2k_2 t)) \quad (35)$$

$$a_g = 1 - \alpha = \frac{1}{2}(1 + \exp(-2k_2 t)) \quad (36)$$

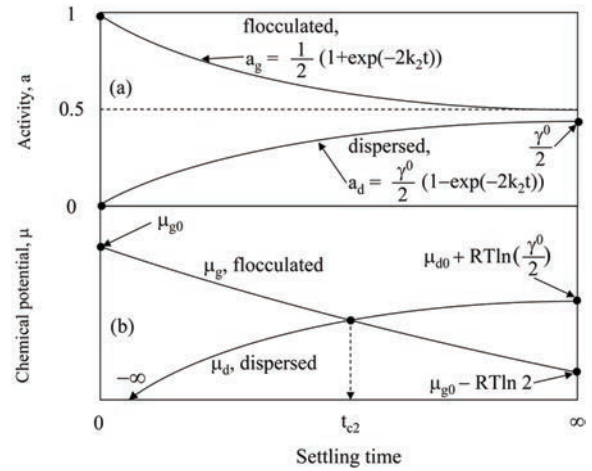


Fig. 10. Activity (a) and chemical potential (b) of dispersed and flocculated particles as a function of settling time.

The chemical potential of dispersed and flocculated particles is expressed by Eqs. (37) and (38), respectively :

$$\mu_d = \mu_{d0} + RT \ln a_d = \mu_{d0} + RT \ln \frac{\gamma^0}{2} (1 - \exp(-2k_2 t)) \quad (37)$$

$$\mu_g = \mu_{g0} + RT \ln a_g = \mu_{g0} + RT \ln \frac{1}{2} (1 + \exp(-2k_2 t)) \quad (38)$$

Equation (39) represents the difference of chemical potential ($\Delta\mu = \mu_g - \mu_d$) :

$$\frac{\Delta\mu}{RT} = \frac{\Delta\mu_0}{RT} - \ln \gamma^0 + \ln \left[\frac{\exp(-2k_2 t) + 1}{\exp(-2k_2 t) - 1} \right] \quad (39)$$

Figure 10 shows the time dependence of activity and chemical potential of dispersed and flocculated particles. The a_g value decreases from 1 at $t = 0$ to 0.5 at $t = \infty$. The a_d increases from 0 at $t = 0$ to $\gamma^0/2$ at $t = \infty$. The corresponding μ_g decreases from μ_{g0} at $t = 0$ to $\mu_{g0} - RT \ln 2$ at $t = \infty$. The μ_d is $-\infty$ at $t = 0$ and increases with an increase of settling time. However, $\Delta\mu$ becomes 0 at $t = t_{c2}$ as seen in Fig. 10(b), and no change of μ_g and μ_d occurs at $t \geq t_{c2}$. The t_{c2} , μ_d , μ_g , and α_c for $\Delta\mu = 0$ are given by Eqs. (40)-(42), respectively:

$$t_{c2} = \frac{1}{2k_2} \ln \left(\frac{\beta + 1}{\beta - 1} \right) = -\frac{1}{2k_2} \ln \tanh \left(\frac{\ln \gamma^0 - \frac{\Delta\mu_0}{RT}}{2} \right) \quad (40)$$

$$\left(\beta \equiv \exp \left(\ln \gamma^0 - \frac{\Delta\mu_0}{RT} \right) \right) \quad (40)$$

$$\mu_g = \mu_d = \mu_{d0} + RT \ln \gamma^0 - RT \ln (\beta + 1) \quad (41)$$

$$\alpha_c = \frac{1}{\beta + 1} \quad (42)$$

The molar fractions of flocculated ($1 - \alpha_c$) and dispersed particles (α_c) at $t = t_{c2}$ are dominated by γ^0 and $\Delta\mu_0$. The difference of $\Delta\mu$ (Eq. (39)) is also expressed by Eq. (43)

using the ratio of t/t_{c2} :

$$\frac{\Delta\mu}{RT} = \frac{\Delta\mu_0}{RT} - \ln \gamma^0 + \ln \left[\frac{\left(\frac{\beta+1}{\beta-1}\right)^{t/t_{c2}} + 1}{\left(\frac{\beta+1}{\beta-1}\right)^{t/t_{c2}} - 1} \right] \quad (43)$$

The thermodynamic condition for stable flocculated particles is $\Delta\mu/RT > 0$ ($\mu_g > \mu_d$). Under this condition, it is difficult to get a well-dispersed suspension. Equation (39) is analyzed for the condition $\Delta\mu/RT > 0$ and the relation expressed by Eq. (44) is reached:

$$t < \frac{1}{2k_2} \ln \left(\frac{\beta+1}{\beta-1} \right) = t_{c2} \quad (44)$$

The rate constant k_2 is expressed by Arrhenius equation (Eq.(45)) :

$$k_2 = k_{20} \exp\left(-\frac{\Delta G_{m2}}{RT}\right) = k_{20} \left(-\frac{\Delta H_{m2}}{RT}\right) \exp\left(-\frac{\Delta S_{m2}}{R}\right) \quad (45)$$

Combination of Eqs.(44) and (45) gives the relation of Eq.(46) :

$$\frac{\Delta H_{m2}}{RT} > \ln \left(2k_{20} \exp\left(\frac{\Delta S_{m2}}{R}\right) \right) + \ln t - \ln \ln \left(\frac{\beta+1}{\beta-1} \right) \quad (46)$$

Figure 11 shows the energy difference of flocculated and dispersed particles at $t < t_{c2}$ and $t = t_{c2}$. The flocculated particles can be released when the bond energy (ΔG_{m2}) between particles is decreased. The corresponding critical ΔH_{m2} is $RT[\ln(2k_{20}\exp(\Delta S_{m2}/R)) - \ln \ln((\beta+1)/(\beta-1))]$ for a fresh suspension ($\ln t \sim 0$) in Eq.(46). Although $\Delta\mu/RT$ is plus at $t < t_{c2}$, the high bond energy prevents the release of flocculated particles and gives the long stability of the flocculated suspension. The difference of stability of dispersed and flocculated suspensions is well understood by the comparison of Figs. 3 and 11. The stability of dispersed particles in Fig. 3 can be increased by increasing ΔG_{m1} . This process is controlled by increasing the surface potential (ϕ) of particles (Fig. 7). On the other hand, the increase of ΔH_{m2} leads to the high stability of flocculated particles (Fig. 11). Unfortunately, the relation between

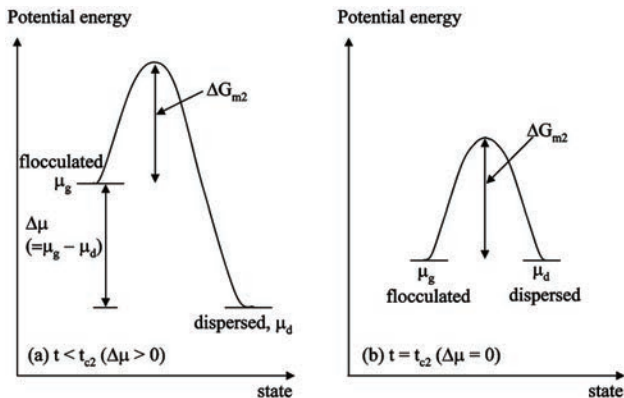


Fig. 11. Energy difference of flocculated and dispersed particles at $t < t_{c2}$ (a) and $t = t_{c2}$ (b).

ΔH_{m2} and ϕ has not been well understood at $\phi < \phi_0$. It may be difficult to disperse the flocculated particles at $t < t_{c2}$ by controlling the surface potential of particles. When the surface potential of flocculated particles is suddenly increased to $\phi > \phi_0$, the chemical potential of dispersed and flocculated particles shifts to the state in Fig. 3(a). In this case the activity of flocculated particles approaches 0, indicating the phase transition from flocculated to dispersed particles (Fig. 2).

The relation between $\Delta H_{m2}/RT$ and $\Delta\mu/RT$ is analyzed for a fresh suspension ($\ln t \ll \ln t_{c2}$). The logarithm term in Eq. (43) can be approximated as follows:

$$\ln \left[\frac{\left(\frac{\beta+1}{\beta-1}\right)^{t/t_{c2}} + 1}{\left(\frac{\beta+1}{\beta-1}\right)^{t/t_{c2}} - 1} \right] = \ln \left[\frac{1 + \left(\frac{\beta-1}{\beta+1}\right)^{t/t_{c2}}}{1 - \left(\frac{\beta-1}{\beta+1}\right)^{t/t_{c2}}} \right] \approx 2 \left(\frac{\beta-1}{\beta+1} \right)^{t/t_{c2}} \quad (47)$$

$\left(0 < \frac{\beta-1}{\beta+1} < 1, 0 < \frac{t}{t_{c2}} < 1 \right)$

Equation (47) is substituted for Eq. (43) to yield Eq. (48):

$$\frac{\Delta\mu}{RT} \approx \frac{\Delta\mu_0}{RT} - \ln \gamma^0 + 2 \left(\frac{\beta-1}{\beta+1} \right)^{t/t_{c2}} \quad (48)$$

Equation (48) was coupled with Eq. (46) to give the relation of Eq. (49) for the conditions of $\Delta\mu/RT > 0$ and $\ln t \ll \ln t_{c2}$:

$$\ln \left[-\ln \left(\frac{\Delta\mu}{2RT} + \frac{\ln \beta}{2} \right) \right] > \ln B - \ln t_{c2} - \frac{\Delta H_{m2}}{RT} \quad (49)$$

where B is $2k_{20} \exp(\Delta S_{m2}/R)$ (See Eq. (46)). Figure 7 shows the relation of $\Delta\mu/RT$ and $\Delta H_{m1}/RT$ for the analysis of section 3 (dispersed \rightarrow flocculated) and section 8 (flocculated \rightarrow dispersed). At $\Delta\mu/RT = 0$, both the enthalpy of ΔH_{m1} in Eq.(25) and ΔH_{m2} in Eq.(49) becomes equal (Eq. (50)) :

$$\frac{\Delta H_{m1}}{RT} = -A - 3 \ln r = \frac{\Delta H_{m2}}{RT} = \ln B - \ln t_{c2} - \ln \left(-\ln \left(\frac{\ln \beta}{2} \right) \right) \quad (50)$$

Equation (50) indicates that (i) a critical ΔH_{m2} is equal to a critical ΔH_{m1} at $\Delta\mu = 0$ and (ii) a critical ΔH_{m2} can be a function of particle size because ΔH_{m1} depends on particle size and (iii) a critical ΔH_{m2} is higher for smaller particles. That is, a higher energy is needed to disperse the flocculated particles of smaller size. Since we have analyzed the critical ΔH_{m1} as a function of particle size in section 6, those values are equal to the critical ΔH_{m2} values at $\Delta\mu/RT = 0$

Packing Behavior of Dispersed and Flocculated Particles

Based on the thermodynamics of colloidal suspensions, we discuss the packing behavior of colloidal particles. Figure 12 shows the schematic phase diagram and the

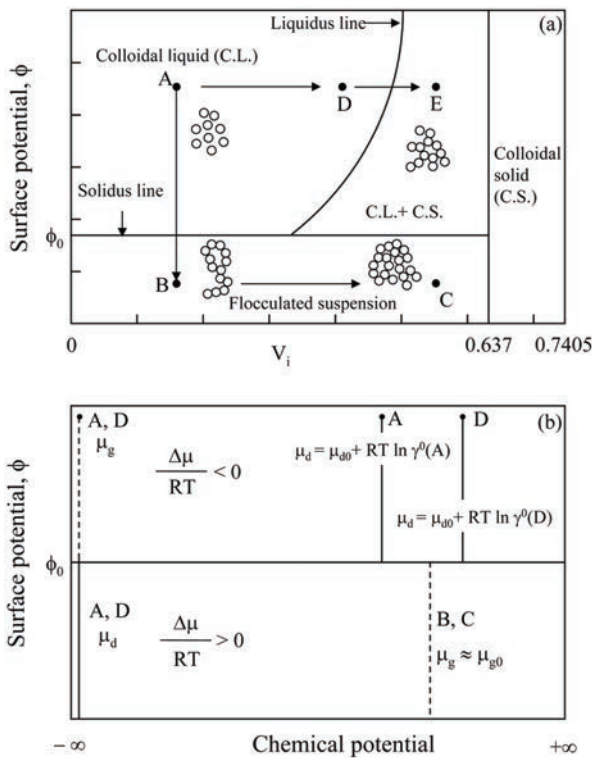


Fig. 12. Colloidal phase diagram (a) and chemical potential (b) of dispersed (A, D) and flocculated particles (B, C) in a fresh suspension.

chemical potential of dispersed and flocculated particles in a fresh colloidal suspension with a small value of k_1 or k_2 (Eqs. (9) and (34)). The μ_g of flocculated particles at the compositions A and D ($\phi > \phi_0$) is $-\infty$ ($a_g \sim 0$) and the μ_d of dispersed particles at the composition A and D is $-\infty$ ($a_d \sim 0$) at $\phi < \phi_0$. The increase of particle content from point A to D causes the increase of μ_d as seen in Fig. 12 (b). In the particle content range above the composition of the liquidus line (point E), colloidal solid and colloidal liquid coexist. However, the distance between two particles in this composition is very small as compared with the particle size, suggesting the formation of a dense powder compact at the liquidus line. That is, the particle content of the liquidus line is interpreted to be a critical packing density of colloidal particles. Further densification in the colloidal solid range corresponds to the disorder-order transformation (crystallization of randomly close-packed particles) [4, 5, 14].

Figure 13 shows the critical packing density determined from the liquidus line at 100 mV (dispersed particles) and at ϕ_0 mV (solidus lines) of surface potential as a function of particle size (See Fig. 8). The packing density of the dispersed particles, determined from the phase diagram, decreases from 58% at 1000 nm to 30% at 10 nm. In the particle size range from 100 to 10 nm, the decrease of the density is significant. However, the packing density at $\phi = \phi_0$ is not sensitive to the particle size and is in the range from 26 to 35 vol%. That is, a porous powder compact is formed. Figure 13 also shows the packing density of ceramic particles with a size of 24–800 nm. The ceramic

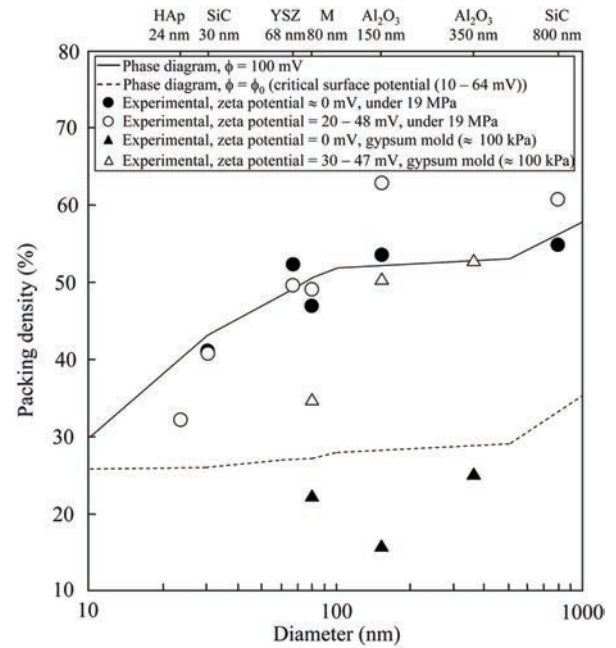


Fig. 13. Packing density of nanometre-sized ceramic particles as a function of particle size. YSZ, HAp, and M represent yttria-stabilized zirconia, hydroxyapatite and mullite, respectively. The seven kinds of colloidal particles were consolidated by pressure filtration at 19 MPa of applied pressure or using gypsum mold.

suspension of 5–20 ml was consolidated by a developed pressure filtration apparatus under a pressure of 19 MPa or using a gypsum mold (suction pressure : 50–100 kPa) [24]. In the experiment, colloidal suspensions at 20–48 mV of zeta potential and at near the isoelectric point (flocculated particles) were consolidated. The detailed experimental procedure is reported in our papers [12, 24–27]. As seen in Fig. 13, the packing densities of the powder compacts consolidated by pressure filtration (~ 19 MPa) of the particles with high and low zeta potentials are very close to the compositions of liquidus lines at 100 mV of surface potential. The surface potential of the particles smaller than 100 nm does not affect the packing density. This result is explained by the shift of the solidus line to a higher ϕ with decreasing particle size. The colloidal suspensions for the particles of 20–70 nm were in a flocculated state at the given zeta potentials. In the submicrometre range, the packing density is influenced by the surface potential and became higher than the compositions of liquidus lines. This result may reflect the crystallization of highly dispersed particles during the consolidation.

The phase diagram constructed is effective to predict the packing behavior of colloidal particles. When the surface potential of particles is decreased from point A to B in Fig. 12, a stable flocculated suspension is formed. According to the phase diagram Fig. 12 (a), the flocculated suspension consists of a mixture of solution and flocculated particles with a packing density of 0.637. The increase of particle content from point B to C at $\phi < \phi_0$ leads to the increased fraction of flocculated particles. This change of the structure provides finally the dense compact with

V_{\max} of packing density. That is, it is possible to make a dense powder compact when the solid content of the flocculated suspension can be increased. The good agreement between the compositions of liquidus lines at 100 mV of surface potential and the experimental packing densities for the flocculated suspensions under a pressure of 19 MPa indicates that (i) the application of external force can increase the particle content of the flocculated suspension, and (ii) the final packing density of the flocculated particles is the same as the density corresponding to the liquidus lines at $\phi > \phi_0$. As seen in Fig. 13, the packing density of the submicrometre-sized alumina powders consolidated by filtration through a gypsum mold is also close to the density predicted from the phase diagram. Application of a high pressure (~19 MPa) during the consolidation enhances the elimination of solution and the disorder \rightarrow order transformation of particles, causing the increase of packing density. A similar consolidation behavior is observed for 80 nm mullite powder with a 30 mV zeta potential. The packing density of this powder is 35 vol% at a low suction pressure (50-100 kPa) but it is possible to increase the density to 49 vol% by increasing the applied pressure. On the other hand, a low packing density of 16-26 vol% was measured for 80-350 nm particles at a 0 mV zeta potential under a low suction pressure. This result is well explained by the density curve determined from the solidus line of the phase diagram. Apparently, the flocculated particles can be consolidated to a high packing density predicted from the phase diagram under a high consolidation pressure. As discussed above, the important processes to increase packing density are the elimination of solution and crystallization of particles during consolidation, which depend on particle size, surface potential and applied pressure.

Conclusions

This paper has defined the activity and chemical potential of dispersed (μ_d) and flocculated (μ_g) particles of a one-component colloidal system. The difference of chemical potential ($\Delta\mu = \mu_g - \mu_d$) for dispersed and flocculated particles provides a critical enthalpy (ΔH_{m1}) for the formation of a particle cluster, which is equal to a certain maximum value of the interaction energy as a function of distance of two particles in the DLVO theory. The combination of thermodynamics of colloidal suspensions and the DLVO theory succeeded in constructing the colloidal phase diagram in a map of surface potential (ϕ) and solid content of particles of 10-1000 nm diameters. The critical enthalpy (ΔH_{m1}) corresponds to the solidus line ($\phi = \phi_0$) of the phase diagram giving $\Delta\mu = 0$. The ϕ_0 value shifts to a higher value with decreasing particle size. The particle composition of liquidus line is also related to the packing density after consolidation of dispersed particles. This phase diagram can predict the dependence of packing density on particle size. The experimentally-determined packing density agreed with the prediction from the phase diagram. The

thermodynamics of the dispersion of the flocculated particles is also discussed. The packing behavior of a flocculated suspension at near the isoelectric point under a compressive pressure is well explained by the colloidal phase diagram.

References

1. F.F. Lange, B.I. Davis and E. Wright, *J. Am. Ceram. Soc.* 69[1] (1986) 66-99.
2. F.F. Lange, *J. Am. Ceram. Soc.* 72[1] (1989) 3-15.
3. I.A. Aksay, F.F. Lange and B.I. Davis, *J. Am. Ceram. Soc.* 66[10] (1983) C190-C190.
4. I.A. Aksay, in "Ceramics: Today and Tomorrow" (The Ceramic Society of Japan, Tokyo, 1986, Edited by S. Naka, N. Soga and S. Kume) pp.71-85.
5. Y. Hirata, A. Nishimoto and Y. Ishihara, *J. Ceram. Soc. Japan* 100[8] (1992) 983-990.
6. J.A. Lewis, *J. Am. Ceram. Soc.* 83[10] (2000) 23-41.
7. J.T.G. Overbeek, in "Colloid Science I" (Elsevier Publishing Company, Amsterdam, 1952, Edited by H.R. Kruyt) pp.245-301.
8. D.J. Shaw, "Introduction to Colloid and Surface Chemistry" (Butterworth, London, 1980) pp.183-212.
9. Y. Hirata, *Ceram. Inter.* 23 (1997) 93-98.
10. Y. Hirata and Y. Tanaka, *Bull. Ceram. Soc. Japan* 42[2] (2007) 87-92 (in Japanese).
11. Y. Hirata, S. Nakagama and Y. Ishihara, *J. Ceram. Soc. Japan* 98[4] (1990) 316-321.
12. Y. Hirata, H. Haraguchi and Y. Ishihara, *J. Mater. Res.* 7[9] (1992) 2572-2578.
13. I.A. Aksay and R. Kikuchi, in "Science of Ceramic Chemical Processing" (John Wiley & Sons, Inc., New York, 1986, Edited by L.L. Hench and D.R. Ulrich) pp.513-521.
14. W.B. Russel, *Mater. Res. Soc. Bull.* XVI[8] (1991) 27-31.
15. V. Deniz, M. Boström, D. Bratko, F.W. Tavares and B.W. Ninham, *Colloids Surf., A Physicochem. Eng.* (2007) 5 pages, Available online.
16. P.C. Zamora and C.F. Zukoski, *Langmuir*, 12 (1996) 3541-3547.
17. S. Ramakrishnan and C.F. Zukoski, in "Dekker Encyclopedia of Nanoscience and Nanotechnology" (Marcel Dekker, Inc. New York, 2004) pp.2813-2824.
18. R.A. Swalin, "Thermodynamics of Solid" (John Wiley & Sons, New York, 1972) pp.119-140.
19. J.M. Ziman, "Models of Disorder" (Cambridge University Press, Oxford, 1979) pp.78-87.
20. W.D. Kingery, H.K. Bowen and D.R. Uhlmann, "Introduction to Ceramics, Second Edition" (John Wiley & Sons, New York, 1976) pp.227-232.
21. H.A. Barnes, J.F. Hutton and K. Walters, "An Introduction to Rheology" (Elsevier Science Publishers, Amsterdam, 1989) p.118.
22. Y. Fukuda, T. Togashi, M. Naitou and H. Kamiya, *J. Ceram. Soc. Japan* 109[6] (2001) 516-520.
23. R.H. Doremus, "Rates of Phase Transformations" (Academic Press, Inc., Orlando, 1985) pp.4-32.
24. Y. Hirata, M. Nakamura, M. Miyamoto, Y. Tanaka and X.H. Wang, *J. Am. Ceram. Soc.* 89[6] (2006) 1883-1889.
25. K. Kishigawa and Y. Hirata, *J. Ceram. Soc. Japan* 114[3] (2006) 259-264.
26. Y. Hirata and Y. Tanaka, in Proceedings of 6th Pacific Rim Conference on Ceramic and Glass Technology-Pacrim 6, October 2006 (The American Ceramic Society (CDR)).
27. Y. Hirata, Y. Tanaka and Y. Sakamoto, *Adv. Sci. Tech.* 45 (2006) 471-478.